EUROPEAN ORGANIZATION FOR NUCLEAR RESEARCH

Proposal to the ISOLDE and Neutron Time-of-Flight Committee

Nuclear quadrupole moments and charge radii of the $_{51}$Sb isotopes via collinear laser spectroscopy

October 5, 2016

Z.Y. Xu[1], D.T. Yordanov[2], D.L. Balabanski[3], J. Billowes[4], M.L. Bissell[4], K. Blaum[5], B. Cheal[6], S. Malbrunot-Ettenauer[7], S. Franchoo[2], R.F. Garcia Ruiz[4], G. Georgiev[8], W. Gins[1], C. Gorges[9], H. Heylen[5], A. Koszorús[1], S. Kaufmann[9], J. Krämer[9], M. Kowalska[7], G. Neyens[1], R. Neugart[5,10], L. V. Rodriguez [2], W. Nörtershäuser[9], R. Sánchez[11], C. Wraith[6], L. Xie[4], and X.F. Yang[1].

[1]*KU Leuven, Instituut voor Kern-en Stralingsfysica, B-3001 Leuven, Belgium*
[2]*Institut de Physique Nucléaire, CNRS-IN2P3, Université Paris-Sud, Université Paris-Saclay, 91406 Orsay, France*
[3]*ELI-NP, Horia Hulubei National Institute for R&D in Physics and Nuclear Engineering, 077125 Magurele, Romania*
[4]*School of Physics and Astronomy, The University of Manchester, Manchester, M13 9PL, UK*
[5]*Max-Plank-Institut für Kernphysik, D-69117 Heidelberg, Germany*
[6]*Oliver Lodge Laboratory, Oxford Street, University of Liverpool, L69 7ZE, United Kingdom*
[7]*Physics Department, CERN, CH-1211 Geneva 23, Switzerland*
[8]*CSNSM, CNRS-IN2P3, Université Paris-Sud, Université Paris-Saclay, 91405 Orsay, France*
[9]*Institut für Kernphysik, TU Darmstadt, D-64289 Darmstadt, Germany*
[10]*Institut für Kernchemie, Universität Mainz, D-55128 Mainz, Germany*
[11]*GSI Helmholtzzentrum für Schwerionenforschung, D-64291 Darmstadt, Germany*

Spokesperson: Z.Y. Xu, zhengyu.xu@kuleuven.be
D.T. Yodanov, yordanov@ipno.in2p3.fr
Contact person: H. Heylen, hanne.heylen@cern.ch

CERN-INTC-2016-054 / INTC-P-484
06/10/2016

Abstract:

We propose to study the nuclear electromagnetic moments and charge radii of the Sb isotopes with $N = 61 - 84$ using the collinear laser spectroscopy (COLLAPS) beamline at ISOLDE/CERN. The hyperfine spectra of atomic Sb will be obtained with high resolution. The quadrupole moments in particular will help us understand the systematic deviation of the earlier measured magnetic moments from theories. In addition, the charge-radii changes will shed light on the evolution of the nuclear shell structure across the $N = 82$ shell closure.

Requested shifts: 20 shifts (split into 2 runs).

1 Physics motivation

According to the nuclear shell model picture, the antimony isotopes ($Z = 51$) have one single proton outside the $Z = 50$ shell. This particular configuration gives rise to the single-particle (s.p.) character of the ground and low-lying states of Sb isotopes, presenting a stringent test to various nuclear structure models. In addition, the long isotopic chain allows us to investigate possible shell structure evolution as a function of neutron number, which has been one of the key issues in nuclear structure research since the discovery of the vanishing of neutron magic numbers in exotic nuclei such as ^{12}Be, ^{32}Mg, and ^{42}Si [1–3]. Therefore, it is of great significance to study the ground-state (g.s.) properties of the Sb isotopes via collinear laser spectroscopy, which can simultaneously provide nuclear spins, electromagnetic moments, and charge radii.

1.1 Nuclear spins and electromagnetic moments

In odd-even nuclei without strong deformation (not far from a closed shell), the g.s. spins and parities are mostly determined by the s.p. orbit occupied by the last unpaired nucleon. Thus, they are regarded as efficient probes to address the s.p. orbit evolution in a major shell (e.g. odd-mass Cu isotopes [4]). Along the Sb isotopic chain, it has been known that the g.s. spin and parity change to $7/2^+$ from ^{123}Sb onwards, while it is $5/2^+$ in the lighter odd-mass isotopes. According to the nuclear shell models, this modification is ascribed to the mass-dependent nucleon spin-orbit interaction, which leads to the reordering of the two lowest proton s.p. orbits, $d_{5/2}$ and $g_{7/2}$, outside the $Z = 50$ closed shell around $N = 71$ [5]. Experimentally, the g.s. spins/parities are directly measured for $^{113-129}$Sb ($N = 62 - 78$) using proton transfer reactions from the neighboring stable Sn or Te isotopes [6]. Other known values such as that of ^{131,133}Sb [7] are tentatively assigned from the logft values obtained in β-decay experiments or from the extrapolation of systematics (indicated by parenthesis in Table 1). Since g.s. spin and parity are of great importance to understand nuclear structure (for instance to discuss shell evolution or to assign spin/parity in β-decay experiments), it is essential to remeasure the spin of these ground states directly via high-resolution laser spectroscopy to verify previous assignments with more concrete results.

Compared to spins, nuclear magnetic moments μ and quadrupole moments Q are more sensitive to the microscopic configuration of the corresponding state, providing more insight information on the wavefunction of interest. More specifically, the nuclear g factor (defined as $\mu = Ig\mu_N$) is very sensitive to which orbit is occupied by the valence nucleon outside an inert core, whereas the quadrupole moment is more sensitive to collective deformation and core polarization [8]. Experimental data of the g.s. g factors and Q values to date are summarized for the odd-even Sb isotopes in Figs. 1-2. The change of g.s. spin from 5/2 to 7/2 at $N = 71$ is clearly visible in Fig. 1. As reference, the free nucleon Schmidt value $g_{\rm sp}$ (with $g_{s,\pi} = 5.587$ and $g_{l,\pi} = 1$) and the effective s.p. g factor $g_{\rm eff}$ ($g_{s,\pi} = 5.587 \times 0.7$ and $g_{l,\pi} = 1$) for the proton $d_{5/2}$ and $g_{7/2}$ s.p. orbits (predicted by the shell models the two lowest proton s.p. orbits beyond the $Z = 50$ shell) are indicated in the same figure. It can be seen that both calculations reasonably agree with the experimental data, suggesting the proton $d_{5/2}$ or $g_{7/2}$ orbits as the leading configuration. However, it is

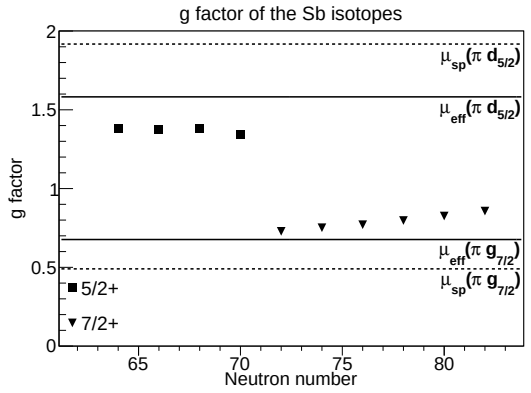

Figure 1: The ground-state g factors of the Sb isotopes with $N = 64 - 82$. All the experimental values are taken from Ref. [11]. As a purpose of comparison, the s.p. Schmidt values $g_{\rm sp}$ (with $g_{s,\pi} = 5.587$ and $g_{l,\pi} = 1$) and effective s.p. values $g_{\rm eff}$ (with $g_{s,\pi} = 5.587\times0.7$ and $g_{l,\pi} = 1$) are indicated for the proton $d_{5/2}$ and $g_{7/2}$ s.p. orbits.

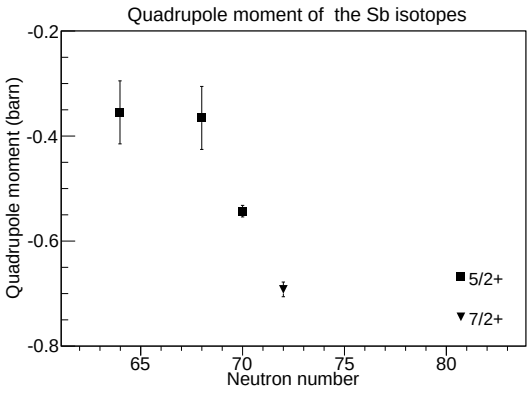

Figure 2: The g.s. quadrupole moments of the odd-even Sb isotopes with $N = 64 - 72$. The data of ^{117}Sb (0.2 ± 1.2 barn [12]) is not plotted on the figure because of its unknown sign and large uncertainty. All the experimental values are taken from Ref. [12, 13].

noteworthy that the discrepancy between the experimental g factors of the $7/2^+$ ground states and the theoretical values becomes greater when the neutrons gradually fill up the $N = 82$ shell. This fact is different from the general case that the prediction with s.p. configuration achieves the best agreement to experimental data when there is only one proton outside a doubly closed shell. In Ref. [7], the authors well reproduced the experimental data by taking into account the contribution of particle-hole excitation in the g.s. wavefunction of the inert core ^{132}Sn. The smooth increase in g factors as the closed shell value $N = 82$ is approached, in a direction away from the Schmidt limit, indicates this core polarization is getting strong towards $N = 82$. Indeed the single-particle character of low-lying levels in Sb isotopes is a controversial issue. The authors in Ref. [9] conclude that the spectroscopic factor of the first $7/2^+$ state exhibits near-single-particle-like character in the Sn(α, t) transfer reactions. In contrast, the shell model calculation with the full $1d_{5/2}$-$0g_{7/2}$-$0h_{11/2}$-$2s_{1/2}$-$1d_{3/2}$ model space reduces the spectroscopic factors of $7/2^+_1$ to $\sim$0.6 for $^{113-125}$Sn [10], suggesting considerable mixing of different configurations in the state. In order to answer the question and pin down the microscopic configuration of the Sb ground states, it is worthy to investigate the quadrupole moments of these states, which give additional information on nuclear deformation and collectivity. Unfortunately, so far the g.s. Q values along the $Z = 51$ chain are very scarce. One can see from Fig. 2 that experimental data is only available till $N = 72$, and the evolution towards $N = 82$ remains unknown. In addition, neither μ or Q has been measured beyond the $N = 82$ shell gap, where different systematics may emerge due to the filling of neutron s.p. orbit $f_{7/2}$ or $h_{9/2}$ outside the closed shell. Therefore, we propose to measure the g.s. quadrupole moments of $^{125-135}$Sb and magnetic moment of ^{135}Sb. The newly measured electromagnetic moments, together with previous data shown in Figs. 1-2, will complement our knowledge on the evolution of core polarization and collectivity towards and beyond the

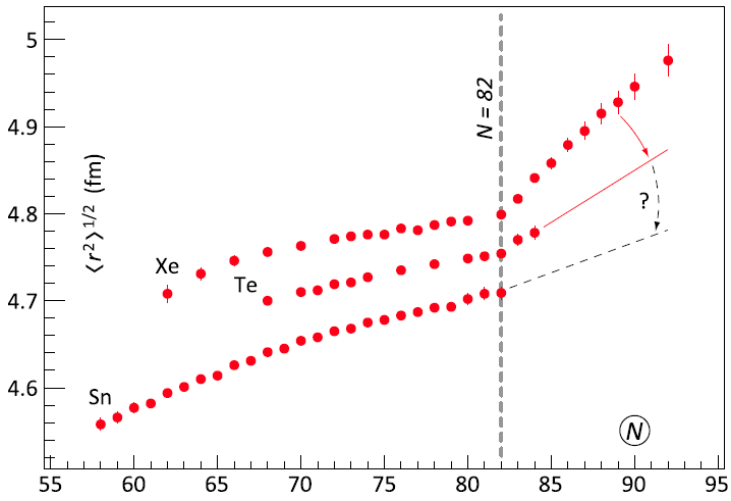

Figure 3: Root mean-square (rms) charge radii of the Xe, Te, and Sn isotopes.

neutron shell closure along the $Z = 51$ isotopic chain.

To have an overview of what has been measured and what can be measured, existing data on nuclear spins and moments relevant to the proposal are summarized in Table 1. It is noted that not only the ground states but also long-lived isomers are accessible by the collinear laser spectroscopy. These isomers can be measured simultaneously with the ground states, providing complementary information to understand the nuclear structure in this region.

1.2 Charge radii

The nuclear charge radius is very sensitive to nuclear size and shape, reflecting the evolution of nuclear structure across the nuclear chart. For instance, a recent work published by Yang *et al.* discovered the shape coexistence in the ^{78}Ni region by measuring the isomer shift in ^{79}Zn [19]. It is also known that the systematics of root mean-square charge radii usually shows a different trend at a shell gap. As illustrated in Fig. 3, the charge radii of Xe isotopes exhibit a well pronounced kink at the shell closure, which is a typical behavior when crossing a strong shell gap [14]. However, the experimental data on the Te ($Z = 52$) isotopes indicates a weakening of this effect, with a decreasing number of valence protons [15]. A similar decrease in the slope of the kink can be seen at $N = 126$ in the Pb region [16], but is not seen at the $N = 28$ shell gap towards doubly magic ^{48}Ca [17]. To better understand the feature and its underlying mechanism, more data on nuclear charge radii crossing a shell gap is required. The measurement on the Sn isotopes beyond $N = 82$ is ongoing [18]. To extend the discussion to odd-proton systems, it is straightforward to build the systematics of Sb isotopes, which fills in the gap between the Te and Sn isotopic chain. So far only the stable Sb isotopes (^{121,123}Sb) have known charge radii and all the unstable isotopes with $N = 61 - 84$ (depending on the production yields, which will be discussed in the Sec. 2) are proposed to be measured.

Table 1: Literature of the Sb isotopes relevant to the proposal. The spin in parenthesis means the value is obtained from indirect measurement such as β-decay experiments or from systematic extrapolation. The data of spin and half life is taken from Ref. [6]. The data of electromagnetic moments is taken from Ref. [11–13]. The abbreviation of methods is listed as follows. NO/S: Static (low-temperature) nuclear orientation; AB: Atomic beam magnetic resonance; NMR/ON: Nuclear magnetic resonance on orientated nuclei; NMR: Nuclear magnetic resonance; NO/D: Dynamic nuclear orientation.

			Magnetic moment		Quadrupole moment	
Nuclide	I^π	$T_{1/2}$	μ (μ_N)	method	Q (barn)	method
^{112}Sb	(3^+)	53.5(6) s				
^{113}Sb	$5/2^+$	6.67(7) min				
^{114}Sb	3^+	3.49(3) min	1.72(8)	NO/S		
^{115}Sb	$5/2^+$	32.1(3) min	+3.46(1)	AB	-0.36(6)	AB
^{116}Sb	3^+	15.8(8) min	2.715(9)	NMR/ON		
^{117}Sb	$5/2^+$	2.80(1) h	+3.43(6)	AB	0.2(12)	AB
^{118}Sb	1^+	3.6(1) min	2.47(7)	AB		
	8^-	5.00(2) h	2.32(4)	NMR/ON		
^{119}Sb	$5/2^+$	38.19(22) h	+3.45(1)	AB	-0.37(6)	AB
^{120}Sb	1^+	15.89(4) min	2.3(2)	AB		
	8^-	5.76(2) d	2.34(1)	NMR/ON		
^{121}Sb	$5/2^+$	stable	+3.3634(3)	NMR	-0.543(11)	O
^{122}Sb	2^-	2.7238(2) d	-1.90(2)	NO/D	+1.28(8)	O
^{123}Sb	$7/2^+$	stable	+2.5498(2)	NMR	-0.692(14)	O
^{124}Sb	3^-	60.20(3) d	1.20(2)	NMR/ON	+2.8(2)	NO/S
	5^+	93(5) s				
	$(8)^-$	20.2(2) min				
^{125}Sb	$7/2^+$	2.75856(25) y	+2.63(4)	NMR		
^{126}Sb	(8^-)	12.35(6) d	1.28(7)	NO/S		
	(5^+)	19.15(8) min				
	(3^-)	about 11 s				
^{127}Sb	$7/2^+$	3.85(5) d	2.697(6)	NMR/ON		
^{128}Sb	8^-	9.05(4) h	1.3(2)	NO/S		
	5^+					
^{129}Sb	$7/2^+$	4.366(26) h	2.79(2)	NMR/ON		
	$(19/2^-)$	17.7(1) min				
^{130}Sb	(8^-)	39.5(8) min				
	$(4,5)^+$	6.3(2) min				
^{131}Sb	$(7/2^+)$	23.03(4) min	2.89(1)	NMR/ON		
^{132}Sb	$(4)^+$	2.79(7) min				
	(8^-)	4.10(5) min				
^{133}Sb	$(7/2^+)$	2.34(5) min	3.00(1)	NMR/ON		
^{134}Sb	(0^-)	0.78(6) s				
	(7^-)	10.07(5) s				
^{135}Sb	$(7/2^+)$	1.679(15) s				

Table 2: Production yield of the Sb isotopes at ISOLDE [23]. The letter "g" denotes the ground state, and "m" denotes isomeric states.

A	112-g	113-g	114-g	114-g	131-g	132-m	133-g	134-g
Target	Ta	UC_x	Ta	UC_x	UC_x	UC_x	UC_x	UC_x
Yield (ions/μC)	2.5E+4	1.1E+7	2.8E+3	6.0E+7	3.2E+9	1.0E+8	1.3E+7	6.0E+6

2 Experimental method

Nuclear spins, electromagnetic moments and changes in mean-square charge radii will be extracted from the hyperfine structure (HFS) of Sb isotopes measured using standard collinear laser spectroscopy on bunched beams at the COLLAPS beamline (details can be found in previous work such as [19]). The fast ion beam delivered from ISOLDE (and bunched using the ISCOOL cooler/buncher) will be neutralized in a potassium-vapor-filled charge exchange cell (CEC) to populate the atomic state of interest for laser spectroscopy. The resulting atomic beam is then excited by the narrow line width continuous wave laser. Fluorescence photons are detected using four photomultiplier tubes (PMTs), each with a large solid-angle acceptance.

To have an idea on which atomic states in Sb will be populated, simulations of the charge exchange process of ionic Sb beams on K vapor have been carried out. The calculations use the model of Rapp and Francis [20] and take into account the redistribution of populated states after the 40-cm transport between the CEC and the optical detection region [21]. According to the simulation, about 19% of the total population is carried by the atomic ground state $(5s)^2(5p)^3\ {}^4S_{3/2}$. Since this study focuses on both quadrupole moments and charge radii, we propose to perform laser spectroscopy on the $(5s)^2(5p)^3\ {}^4S_{3/2} \rightarrow (5s)^2(5p)^2(6s)\ {}^2P_{3/2}$ atomic transition at 45945.34 cm^{-1} (217.58 nm in Air). The field shift factor is appreciable due to the unpaired s-electron of the upper state, and also the hyperfine B parameter is reasonable ($\approx$ 480 MHz in ^{121}Sb) [22].

The published yields of antimony [23] have only been measured with the 0.6-GeV primary beam from the CERN synchrocyclotron (SC) (see Table 2). Below we discuss the relevant intermediate steps in order to arrive at realistic estimates for the production rates expected from the 1.4-GeV beams of the proton synchrotron booster (PSB) while using the resonant ionization laser ion source (RILIS). For this purpose one may look at the production of tin, in particular ^{132}Sn has been measured at the rate of 3×10^7 ions/μC [23] with the SC while the current production [24] with the PSB+RILIS is given at 3×10^8 ions/μC. In the case of antimony this factor of ten is compensated by the difference in efficiency for laser ionization, respectively 22% and 2.7% for tin and antimony [25]. Therefore, one can safely conclude that the SC yields of antimony [23] are consistent with the current production.

The next step is to consider the isobaric contamination which is mostly coming from cesium. Since the cesium is mostly produced by spallation and not fission it is highly beneficial to use a "neutron converter". This will affect the production of antimony which will drop by a factor between 3 and 10. On the conservative side one may adopt the factor of 10 and start examining the case of ^{134}Sb. The SC yield of the latter is 6×10^6 ions/μC, which will drop to about 6×10^5 ions/μC with protons on the converter. This is still approximately two orders of magnitude higher than the sensitivity limit for bunched-beam

collinear laser spectroscopy of minimum required 10^4 ions/μC. It is therefore realistic to consider the feasibility of measuring even the heavier isotopes. Looking at the tin isotopes one makes the conclusion that after the shell closure the addition of one neutron causes the yield to drop by about one order of magnitude, meaning that in terms of production ^{135}Sb and ^{136}Sb should still be within the sensitivity limit stated above. Of course one needs to consider the increase of the contamination. This will not be critical for ^{135}Sb because the production will be an order of magnitude higher than the sensitivity limit, therefore one can afford to reduce the total beam using the slits in order to compensate for the expectedly similar increase in the cesium production. To a certain extent the high-resolution mass separator (HRS) will also play a role in the beam purification.

In short, ^{134}Sb is feasible in terms of production. Recent measurements on ^{134}Sn showed that the isobaric contamination from a UC_x target with proton-beam impinging on a neutron converter is within acceptable limits. In this respect ^{135}Sb is feasible as well because of the available margin for using the HRS slits to compensate effectively for the expected increase of the cesium contamination. Further progress is possible only by additional means of beam purification. We have been informed that in general using a quartz transfer line for trapping the less volatile cesium products is in principle possible. We are very interested in this option, as it may open the possibility to measure ^{136}Sb.

We would like to comment the possibility of reaching some of the neutron-deficient cases, although relevant information on the production rates is somewhat limited. To our knowledge ^{112}Sb has been detected from an oxide target with a FEBIAD (MK5) ion source at the rate of 10^5 ions/μC [26]. This yield is an order of magnitude higher than the sensitivity limit of our technique. Similar to tin, more appropriate target material may be LaC but we are not aware at this time of existing yield estimates from such unit. However, we would like to make an assessment of the applicability of a standard UC target. As stated above in relation to the IS573 experiment, we have been able to measure ^{109}Sn with relative ease by applying the proton beam directly on target. This means that ^{109}Sn must have been produced above the level of 10^5 ions/μC. With respect to antimony, this is a very strong indication that 10^4 ions/μC should be expected around the same mass if the lifetimes are longer than the respective release time. It is, therefore, reasonable to assume that the yield of 10^4 ions/μC can be achieved for isotopes with half lives over a minute, hence a UC target should be applicable for ^{112}Sb and the heavier isotopes. Perhaps we are over conservative here, since the stated SC yield of ^{113}Sb is over 10^7 ions/μC (see Table 2), three orders of magnitude higher than needed for the proposed measurements.

3 Beam-time request

Considering that the production rates of Sb are not publicly available, although accurate data might be available in conjunction with previous measurements such as Arndt *et al.* [27], we have been able to justify the feasibility of the proposed work based solely on existing information. In terms of beam-time estimate it is worth mentioning that laser spectroscopy is not a typical counting experiment and a number of experimental procedures need to be factored in when calculating the likely length of a particular measurement. Some for these considerations are discussed below. One can see from Table 1

that all the isotopes relevant to this proposal have states of non-zero spins, meaning that the measurement will take some time to scan all the peaks in the HFS. For each isotope we want to measure at least three independent HFS scans, and we need also at least one measurement on a reference isotope in order to extract isotope shifts. This means that typically we need $0.5 \sim 1$ shift to measure the HFS scans and reference scans for one isotope that has a yield greater than 10^5 ions/μC (with protons on converter). For the isotope coming at a rate equal or less than 10^5 ions/μC, the typical time is about $1 \sim 1.5$ shifts. Considering there are more than 30 long-lived states that can be measured, we request 20 shifts to establish for the first time

- the ground- and isomeric state spins of the odd-odd and a few odd-even neutron-rich Sb isotopes, and confirm earlier measured spins;
- the quadrupole moments for the neutron-rich isotopes (odd-even and odd-odd);
- the charge radii, with the aim to go beyond $N = 82$ to investigate the slope of the kink.

These shifts will be distributed evenly among two runs, with 2 shifts of stable beam for calibration measurements before each run.

Summary of requested shifts: 18 shifts of radioactive beam and 2 shifts of stable beam are requested for the study of the antimony isotopes $^{112-135}$Sb.

References

[1] H. Iwasaki *et al.*, Phys. Lett. B **481**, 7 (2000);

[2] T. Motobayashi *et al.*, Phys. Lett. B **346**, 9 (1995);

[3] B. Bastin *et al.*, Phys. Rev. Lett. **99**, 022503 (2007);

[4] K.T. Flanagan *et al.*, Phys. Rev. Lett. **103**, 142501 (2009);

[5] A. Bohr and B. Mottelson, Nuclear structure, vol. **1**, Benjamin, New York (1969);

[6] http://www.nndc.bnl.gov/ensdf/, (2016);

[7] N.J. Stone, Phys. Rev. Lett **78**, 820 (1997);

[8] G. Neyens, Rep. Prog. Phys. **66**, 633 (2003);

[9] J.P. Schiffer *et al.*, Phys. Rev. Lett. **92**, 162501 (2004);

[10] Y. Utsuno *et al.*, EPJ Web of Conferences **66** , 02106 (2014);

[11] T.J. Mertzimekis *et al.*, Nucl. Instrum. Meth. Phys. Res. A **807**, 56 (2016);

[12] N.J. Stone, INDC(NDS)-0650 (2013);

[13] P. Raghavan, Atomic data and nuclear data tables **42**, 189 (1989);

[14] P. Campbell, I.D. Moore, and M.R. Pearson, Prog. Part. Nucl. Phys. **86**, 127 (2016);

[15] R. Sifi *et al.*, Hyp. Interact. **171**, 173 (2007);

[16] T.E. Cocolios *et al.*, Phys. Rev. Lett. **106**, 052503 (2011);

[17] K. Kreim *et al.*, Phys. Lett. B **731**, 97 (2014);

[18] D.T. Yordanov *et al.*, Proposal to the ISOLDE and NTFC, (2013).

[19] X.F. Yang *et al.* Phys. Rev. Lett. **116**, 182502 (2016);

[20] D. Rapp and W.E. Francis, The Journal of Chemical Physics **37**, 2631 (1962);

[21] A. Vernon *et al.*, Private communication (2016);

[22] F. Hassini *et al.*, J. Opt. Soc. Am. B **5**, 2060 (1988);

[23] H.-J. Kluge (editor) ISOLDE Guide for Users, CERN 86-05 (1986);

[24] U. Köster *et al.*, Nucl. Instr. Methods B **266**, 4229 (2008);

[25] RILIS online database, http://riliselements.web.cern.ch/riliselements/;

[26] ISOLDE target group, private communication;

[27] O. Arndt *et al.*, Phys. Rev. C **84**, 061307(R) 2011.

Appendix

DESCRIPTION OF THE PROPOSED EXPERIMENT

The experimental setup comprises:

Part of the	Availability	Design and manufacturing
COLLAPS	☒ Existing	☒ To be used without any modification

HAZARDS GENERATED BY THE EXPERIMENT:
Hazards named in the document relevant for the fixed COLLAPS installation.

Additional hazards: no additional hazards.